JOURNAL OF SOLID STATE CHEMISTRY 105, 161–170 (1993)

Crystallographic, Magnetic, and Electrical Properties of $SrTi_{1-x}Ru_xO_3$ Perovskite Solid Solutions

S. L. CUFFINI, V. A. MACAGNO, AND R. E. CARBONIO

Instituto de Investigaciones en Fisicoquímica de Córdoba (INFIQC), Departamento de Físico Química, Facultad de Ciencias Químicas, Universidad Nacional de Córdoba, Sucursal 16, C.C. 61, 5016 Córdoba, Argentina

AND A. MELO, E. TROLLUND, AND J. L. GAUTIER

Departamento de Química, Facultad de Ciencia, Universidad de Santiago de Chile (USACH), C.C. 5659, Santiago 2, Chile

Received December 23, 1991; in revised form January 20, 1993; accepted January 22, 1993

The perovskite compounds $SrTiO_3$ (semiconductor, cubic, and diamagnetic) and $SrRuO_3$ (metallic conductor, orthorhombic, and ferromagnetic) form a continuous series of solid solutions of the formula $SrTi_{1-x}Ru_xO_3$. Increasing substitution of titanium by ruthenium led to a change in the crystallographic, magnetic, and electrical properties. As x increased the latter properties changed from semiconductor to metallic at x values between 0.40 and 0.50. A change from cubic to orthorhombic structure was also observed in the same compositional range as the Ru content increased. The compounds with $x = 1.00$, 0.80, 0.50, and 0.33 obeyed the Curie–Weiss law, with the Weiss constant (θ) and Curie constant (Cm) decreasing as x decreased.

Introduction

Perovskite-type oxides, of the general formula ABO_3, have long been studied because they exhibit physical properties of technological interest (*1–3*). The large variety of properties that these compounds show is derived from the fact that over 90% of the natural metallic elements of the periodic table are known to be stable in a perovskite oxide structure and also from the possibility of synthesis of multicomponent perovskite compounds by partial substitution of cations in A and B positions, giving rise to compounds of the general formula $A_{1-y}A'_yBO_3$ or $AB_{1-x}B'_xO_3$, where A' and B' are cations substituted in the A site and the B site, respectively. The possibility of partial substitution in both A and B positions provides a wealth of isomorphic compounds, giving rise to an extensive range of possibilities in the tailoring of their chemical and physical properties (*4*). Thus, perovskites are ideal for the design of new materials.

The probability of solid solution formation in the entire compositional range is very large when the cation (A or B) is substituted by another cation (A' or B') which has the same charge and a similar ionic radius (*1*, *2*). On the other hand, when there is a large difference, either in charge or in ionic radius, ordered structures are formed, and only certain compositions are allowed (*1*, *2*). Solid solution formation in the entire compositional range has been observed in Ru- or Ti-containing perovskites by partial substitution in the A or B site (*5–11*).

Other interesting properties of perovskites are related to the stability of mixed oxidation states or unusual oxidation states in the structure that make these compounds very useful for catalytic purposes (*12–15*).

0022-4596/93 $5.00

Strontium titanate ($SrTiO_3$) has a cubic perovskite structure at room temperature (*16, 17*) and it is a semiconductor (*18*). The other end member, strontium ruthenate ($SrRuO_3$), has an orthorhombic structure with a slightly distorted unit cell (*19–22*), it is a metallic conductor, and its electrical properties have previously been reported for sintered powders and single crystals (*20, 21, 23*). Its magnetic properties have also been studied and are particularly interesting since $SrRuO_3$ represents the first example of ferromagnetism resulting only from a second-row transition element (*24–27*).

Reller (*11*) reported that $SrRuO_3$ and $SrTiO_3$ were able to form solid solutions for all the Ru : Ti ratios; however, no detailed structural studies were reported.

This paper deals with the preparation and characterization of a continuous series of solid solutions of the formula $SrTi_{1-x}Ru_xO_3$ (x = 0.00, 0.10, 0.33, 0.35, 0.40, 0.50, 0.80, and 1.00). Due to the different properties of the end members, the $SrTi_{1-x}Ru_xO_3$ solid solution offers the interesting possibility of tailoring electrical, magnetic,and crystallographic properties. For this reason, the effects of the substitution of titanium by ruthenium on those properties are systematically investigated.

Experimental

Synthesis

$SrRuO_3$ was prepared by solid-state synthesis. Intimately mixed appropriate amounts of $SrCO_3$ (Mallinckrodt) and RuO_2 (99.99%, Aldrich) were ground in an agate mortar. The mixture was heated in air for 3 hr at 1100°C. $SrTiO_3$ was prepared by mixing $TiCl_4$ (Carlo Erba, R P) with $Sr(NO_3)_2$ (Cicarelli, P.A.) in aqueous solution in stoichiometric amounts; then a solution containing NH_4OH and $(NH_4)_2CO_3$ was added while stirring until precipitation was complete. The solid product was then filtered, washed with water, dried at 120°C, and heated in air for 3 hr at 1100°C.

Samples containing titanium and ruthenium in different ratios ($SrTi_{1-x}Ru_xO_3$ with x = 0.10, 0.33, 0.35, 0.40, 0.50, and 0.80) were prepared by the following procedure. The intimate mixture of strontium and titanium in the Sr : Ti ratio 1: (1 − x) was prepared as mentioned above for $SrTiO_3$. Then the appropriate quantity (x) of RuO_2 was added and the materials were ground in agate mortar. The mixture was heated in air at 1100°C for 3 hr.

$SrTiO_3$ is white and $SrRuO_3$ is black, while the samples with x = 0.10, 0.33, 0.35, and 0.40 are brown and those with x = 0.50 and 0.80 are black. Some of these results are in agreement with the observation that $SrTi_{0.95}Ru_{0.05}O_3$ is dark brown (*11*).

Chemical Analysis

In order to determine the accurate composition of the different compounds, they were analyzed with a plasma emission spectrophotometer (SOBIN-IVON, Model JY38 type 2).

Since a sufficient amount of the oxides must be completely dissolved in order to perform the analyses, different solvents were tested. Total or partial insolubility was observed in cold and boiling HNO_3, HCl, aqua regia, H_2SO_4, and KOH for all compositions. Complete dissolution of the sample was obtained only by performing the chemical attack in a metallic piston with a Teflon vessel, which allows one to work under pressure and at high temperatures. Approximately 30 mg of the sample was added to 2 ml of aqua regia and 6 ml of HF, and the closed system was heated at 120°C for several hours. For the samples with x = 0.00, 0.10, 0.33, 0.35, and 0.40 this temperature was maintained for 2 hr and for x = 0.50, 0.80, and 1.00 for 8 hr. Considering the experimental errors,the compositions of all the compounds are in good agreement with the expected ones.

From these results it can be concluded that these oxides may be used where moderate or hard acid media are necessary, since they are extremely resistant to chemical attack.

TABLE I

CRYSTALLOGRAPHIC DATA FOR $SrTiO_3$ AND $SrRuO_3$

	$SrTiO_3$	$SrRuO_3$
Space group	*Pm3m* (No. 221)[a]	*Pnma* (No. 62)[a]
Cell dimensions		
a	3.9032(2) Å	5.578(1) Å
b		7.842(2) Å
c		5.539(1) Å
Cell volume	59.47(1) Å^3	242.5(1) Å^3
Unit cell contents	$Z = 1$	$Z = 4$
Formula weight	183.518	236.688
Density (calculated)	5.124 g cm^{-3}	6.483 g cm^{-3}

[a] Ref. (*40*).

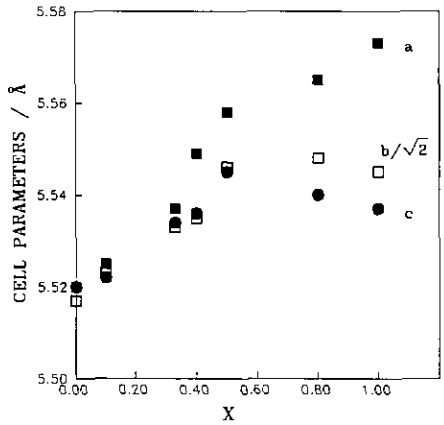

FIG. 1. Lattice parameters of $SrTi_{1-x}Ru_xO_3$ as a function of composition. $b/\sqrt{2}$ is plotted rather than b because cubic symmetry occurs at $a = c = b/\sqrt{2}$.

X-Ray Diffraction

The unit cell parameters of the perovskite structure were determined by Debye–Scherrer powder photographs using Ni-filtered Cu$K\alpha$ radiation and a Philips camera (114.6 mm). X-ray patterns of these oxides were also taken on a Philips powder diffractometer 1050-80 (Cu$K\alpha$ radiation and graphite monochromator).

The X-ray data were processed with the computer programs LATTICE (*28*) and LAZY PULVERIX (*29*).

Scanning Electron Microscopy

Scanning electron microscopy (SEM) using a Philips 505E microscope and energy dispersive absorption of X-ray (EDAX) were used to examine and characterize the powder samples.

Magnetic Measurements

Magnetic measurements were performed by the Faraday method with a magnetic balance (Cahn, Model 7800) in the temperature range 300 to 570 K. The instrument was calibrated with $Hg[Co(CNS)_4]$. The measurements were corrected taking into account the sample holder and sample oxygen diamagnetism.

Electrical Resistivity Measurements

The electrical resistivity measurements were performed with an impedance bridge (Marconi Instruments, Model TF2700) which allows measurements under ac at 1 kHz. Standard two-probe resistivity measurements were made on sintered pellets;

TABLE II

LATTICE PARAMETERS VS COMPOSITION

Formula	*a* (Å)	*b* (Å)	*c* (Å)	*V* (Å^3)
$SrTiO_3$[a]	5.520(1)	7.806(1)	5.520(1)	237.8(1)
$SrTi_{0.90}Ru_{0.10}O_3$	5.525(2)	7.811(3)	5.522(2)	238.3(3)
$SrTi_{0.66}Ru_{0.33}O_3$	5.537(2)	7.825(3)	5.534(2)	239.8(3)
$SrTi_{0.60}Ru_{0.40}O_3$	5.549(3)	7.828(4)	5.536(3)	240.5(4)
$SrTi_{0.50}Ru_{0.50}O_3$	5.558(3)	7.844(4)	5.545(3)	241.7(4)
$SrTi_{0.20}Ru_{0.80}O_3$	5.565(3)	7.849(4)	5.540(3)	242.1(4)
$SrRuO_3$	5.578(1)	7.842(2)	5.539(1)	242.5(1)

[a] Transformed unit cell; see text.

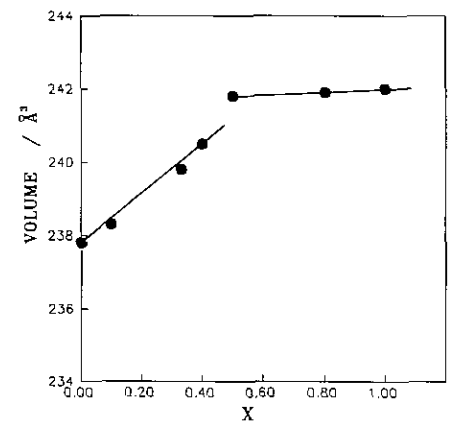

FIG. 2. Cell volume of $SrTi_{1-x}Ru_xO_3$ as a function of composition.

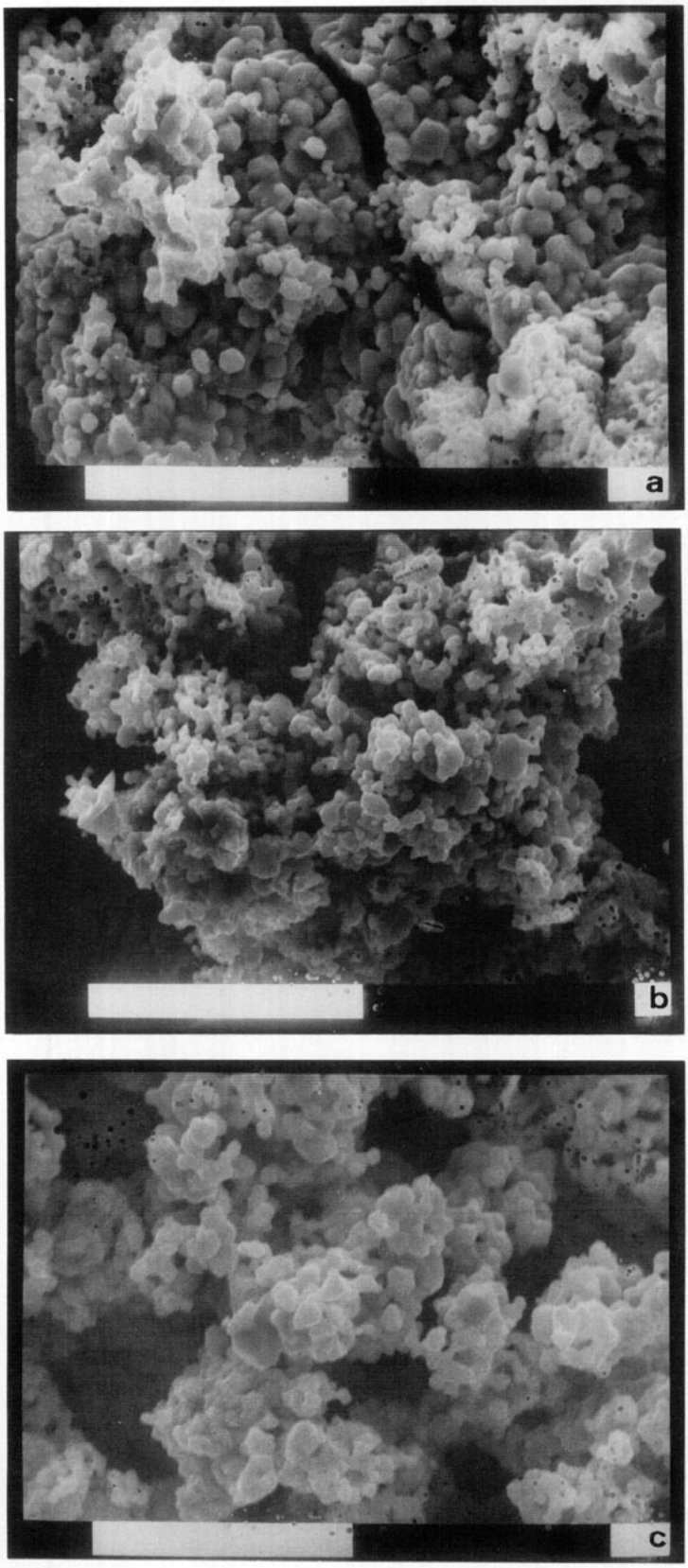
a
b
c

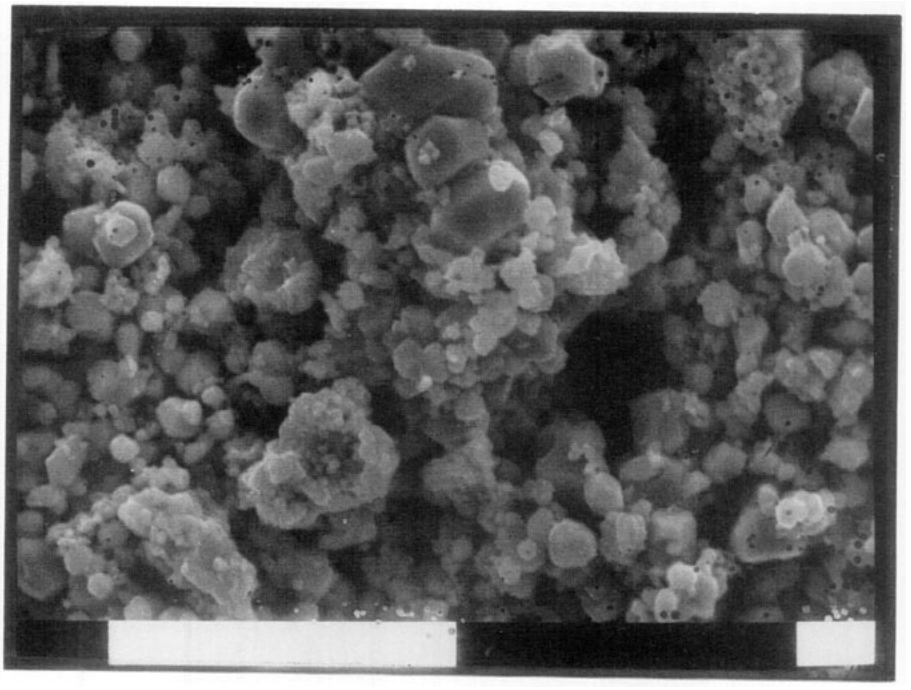

FIG. 4. SEM microphotograph of a $SrRuO_3$+ $SrTiO_3$ mixture. Scale, 10 μm.

the oxides were pressed into disks at 5 tonne cm^{-2} and sintered for 6 hr at 1100°C in air. For the sintered samples, intimate electrical contact between the copper pistons and the pellet was provided by using silver paint.

The temperature was varied in the range 300 to 450 K and during a typical run, the sample resistivity was measured at intervals of about 1–5 K.

IR Measurements

Infrared spectra were recorded on a FTIR spectrometer (NICOLET 5 SXC) at room temperature. The compounds (1 wt%) were mixed thoroughly with KBr (Carlo Erba, R P) and pressed into disks 0.5 mm thick.

Results and Discussion

Crystallographic Data

The X-ray powder diffraction patterns showed that the compounds with $x = 0.10$, 0.33, 0.40, 0.50, and 0.80 were all single-phase materials and as there was no evidence of superstructure, they may be assumed to have a random or near-random distribution of Ti and Ru on the *B* sites. This is reasonable, since Ti^{4+} and Ru^{4+} have the same charge and very similar ionic radii, which are the conditions for nonordered solid solution formation as discussed above.

The $SrTiO_3$ pattern could be indexed with a cubic unit cell, whereas the $SrRuO_3$ pattern required an orthorhombic one, since the splitting of back reflection lines could be detected. However, its unit cell is slightly distorted from the one found in the ideal cubic perovskite structure. This distortion is due to a slight tilting of the RuO_6 octahedra (*22*) which leads to the O-orthorhombic type structure, since the lattice-parameter ratio b/c is greater than $\sqrt{2}$ where $c < a$, as described by Goodenough and Longo (*1*). The resulting cell parameters are listed in Table 1 and show good agreement with the available literature values (*8, 9, 16, 20, 22,*

FIG. 3. SEM microphotographs of powder samples with $x = 0$(a), 0.50 (b), and 1.00 (c). Scale, 10 μm.

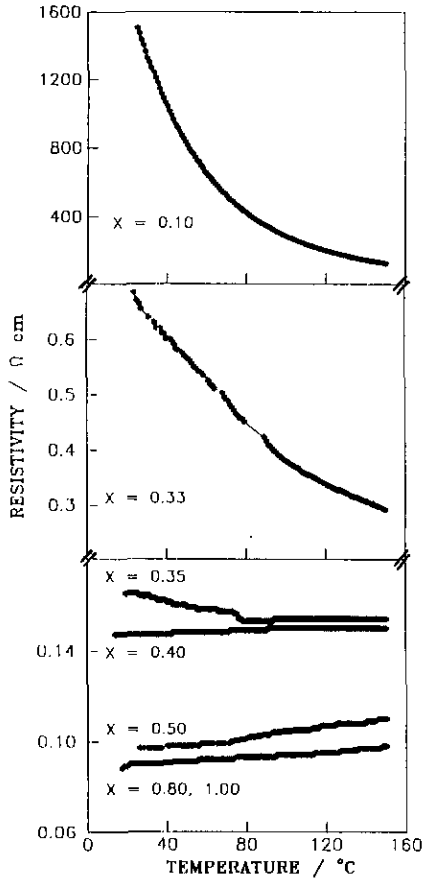

FIG. 5. Electrical resistivity vs temperature of $SrTi_{1-x}Ru_xO_3$ for different compositions (x = 0.10, 0.33, 0.35, 0.40, 0.50, and 1.00).

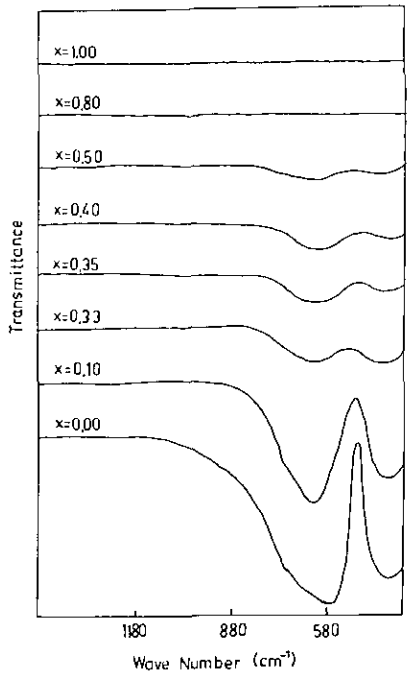

FIG. 6. IR spectra of $SrTi_{1-x}Ru_xO_3$ for different compositions at 298 K.

23). Reller and co-workers (*30*) recently reported a cubic structure for $SrRuO_3$ single crystals; however, this is in disagreement with our results and the other publications mentioned above.

The X-ray patterns of solid solution $SrTi_{1-x}Ru_xO_3$ showed a change from a cubic to orthorhombic structure. To look at this change, it is convenient to transform the cubic unit cell of $SrTiO_3$ by a transformation matrix (101, 020, 101) (*9*) to a cell with parameters $a = c = 5.520(1)$ Å and $b = 7.806(1)$ Å which could be matched with the $SrRuO_3$ unit cell. Lattice parameters vs x are listed in Table II and illustrated in Fig. 1. For $x = 0.10$ and 0.33, $a \cong c \cong b/\sqrt{2}$, which could be attributed to the fact that its unit cell is almost cubic. However, for $x \geq 0.50$, the orthorhombic distortion is considerable. A plot of the cell volume vs

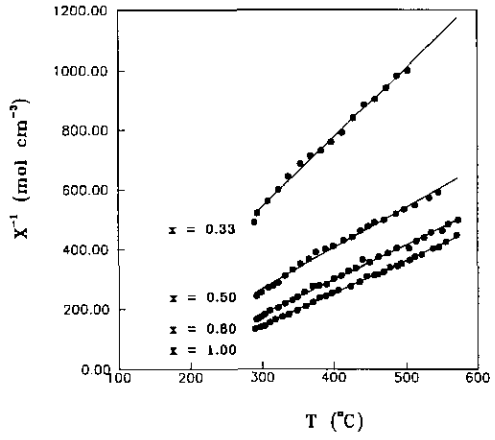

FIG. 7. Reciprocal susceptibility vs temperature of $SrTi_{1-x}Ru_xO_3$ for different compositions (x = 0.33, 0.50, 0.80, and 1.00).

TABLE III

MAGNETIC DATA

Compound	Cm (mole^{-1} K cm^3)	θ (K)
$SrRuO_3$	0.92 ± 0.1	165 ± 4
$SrTi_{0.20}Ru_{0.80}O_3$	0.86 ± 0.01	142 ± 7
$SrTi_{0.50}Ru_{0.50}O_3$	0.74 ± 0.02	102 ± 10
$SrTi_{0.66}Ru_{0.33}O_3$	0.43 ± 0.01	68 ± 9

x (Fig. 2) shows this change more clearly. Two straight lines, with a break between $x = 0.40$ and 0.50, are observed, showing that the cubic to orthorhombic transition occurs in this compositional range.

Figure 3 shows SEM microphotographs of powder samples with different x values. All samples are fine grained and dispersed and the mean grain size is in the range 1–3 μm. The energy dispersive X-ray analysis conducted on different size areas spread over the surface indicated a uniform distribution of Ru and Ti for the samples with $x = 0.10$, 0.33, 0.35, 0.40, 0.50, and 0.80. For comparison, a SEM microphotograph of a mixture of $SrRuO_3$ and $SrTiO_3$ is shown in Fig. 4. The EDAX analysis indicated that the large crystals with regular shapes correspond to $SrTiO_3$ and the small crystals with poorly defined shapes correspond to $SrRuO_3$. A comparison with the results for $x = 0.50$ (Fig. 3) and other x values (not shown) clearly shows that the compounds containing Ru and Ti have a uniform distribution of these elements and crystal sizes and shapes. These results together with the X-ray diffraction measurements indicate that there is a continuous set of solid solutions.

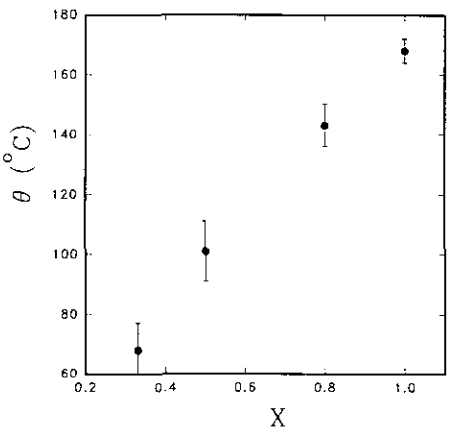

FIG. 8. Weiss constant (θ) of $SrTi_{1-x}Ru_xO_3$ as a function of composition.

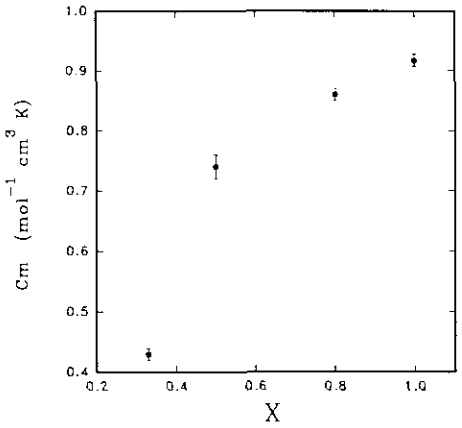

FIG. 9. Curie constant (Cm) of $SrTi_{1-x}Ru_xO_3$ as a function of composition.

Electrical Properties

Figure 5 shows electrical resistivity (ρ) measurements of sintered pellets. The results clearly show that increasing substitution of Ti^{4+} by Ru^{4+} in $SrTiO_3$ causes a decrease in resistivity.

The metallic conduction in $SrRuO_3$ appears to be maintained down to $x = 0.50$. The change from metallic to semiconducting properties with decreasing x is also reflected in the infrared spectra shown in Fig. 6. Infrared spectra of ABO_3 perovskite oxides in the region 300–1000 cm^{-1} have been studied mainly to obtain information at a microscopic level on the nature of metal–oxygen bonding at the metal–insulator (M–I) transition (*31*). The two prominent bands that perovskites generally show in this region are related to the internal modes of the BO_6 octahedra (*32*). The compounds with $x \geq 0.50$ show a continuous absorption characteristic

of a high free carrier concentration, in agreement with the metallic conduction, while the spectra of the compounds with $x < 0.50$ show the development of increasing absorption bands with decreasing x, corresponding to the increase in the semiconducting behavior. Therefore, the M–I transition observed with resistivity measurements is verified with the IR measurements. The M–I transition thus occurs in the same compositional range as the crystallographic transition. This might be considered a Mott transition (*33*), which is first order and is necessarily accompanied by a change in volume and sometimes by a change in structure.

Electrical resistivity in perovskite oxides has been widely discussed (*1, 3, 26, 34, 35*). The overlap of metal *d*-orbitals of t_{2g} symmetry with oxygen *p*Π orbitals leads to the formation of Π*-type conduction bands in $SrTiO_3$ ($Ti^{4+}: t_{2g}$) which are completely empty (*27, 36*) and a semiconducting behavior is observed, with a band gap of 3.2 eV (*37, 38*). Conversely, in $SrRuO_3$ the t_{2g} states of Ru ($Ru^{4+}: t_{2g}$) lead to a metallic conduction band which is two-thirds filled so that metallic conductivity is possible (*24, 25*).

The substitution of Ru^{4+} by Ti^{4+} in the system $SrTi_{1-x}Ru_xO_3$ is expected to produce a break in the conduction pathway within the three-dimensional network of the RuO_6 octahedra, leading to a metal–insulator transition. It is interesting to note that similar behavior has been observed in $SrFe_{x}Ru_{1-x}O_{3-\sigma}$ (*23*), $LaRu_xGa_{1-x}O_3$ (*5*), and $LaRu_xFe_{1-x}O_3$ (*6*). In order to understand the M–I transition and to study the conductivity mechanism of these oxides, resistivity measurements at lower temperatures are currently being performed and will be reported in a future publication.

Magnetic Properties

Magnetic susceptibility was measured as a function of temperature (300–500 K) for all the solid solutions. The $1/X_M$ vs T plots are shown in Fig. 7. Good agreement with the Curie–Weiss law is observed for x = 1.00, 0.80, 0.50, and 0.33 in the covered temperature range. The Weiss constant (θ) and the Curie constant (Cm) calculated by extrapolation decrease with decreasing x (Table III); this is reasonable, since the dilution of a magnetic ion (Ru^{4+}) by a nonmagnetic one (Ti^{4+}) leads to a weakening of the ferromagnetic exchange interaction. Plots of θ and Cm vs x are shown in Figs. 8 and 9 (the bars indicate the standard deviations obtained from error propagation analysis). θ decreases almost linearly with x and Cm decreases almost linearly with x from x = 1.00 to x = 0.50; however, the value for x = 0.33 is significantly smaller than would have been predicted given the other points. The results for x = 0.10 could not be considered since there was a large experimental error in the data because of the low Ru content. The Weiss constant and the effective paramagnetic moment obtained for $SrRuO_3$ (μ_{eff} = 2.70 μ_B) are in good agreement with the literature values (*8, 25, 39*). More detailed magnetic susceptibility and ESR measurements are in progress.

Conclusions

$SrTiO_3$ and $SrRuO_3$ form a continuous series of solid solutions with the general formula $SrTi_{1-x}Ru_xO_3$ for all x values. Crystallographic, magnetic, and electrical properties change with x. The crystalline structure changes from a simple cubic structure for x = 0.00 to an orthorhombic one for x = 1.00. The cubic to orthorhombic transition occurs between x = 0.40 and 0.50.

The compounds with x = 1.00, 0.80, and 0.50 exhibit typical metallic behavior and those with x = 0.10, 0.33, 0.35, and 0.40 are semiconductors in the temperature range covered in the present paper. The resistivity measurements show a M–I transition between x = 0.40 and 0.50 which is also verified with IR measurements. This transition thus occurs in the same compositional range in which the cubic to orthorhombic transition occurs.

The Weiss constant (θ) and Curie constant

(Cm) decrease with x, indicating a weakening of the ferromagnetic exchange interactions.

All the compounds are very insoluble in acidic solutions such as concentrated HNO_3, HCl, aqua regia, or H_2SO_4 and in concentrated KOH; so these compounds could be of interest in applications where stability in these media is required, such as in electrodes for electrochemical cells.

Acknowledgments

Financial support from the Consejo Nacional de Investigaciones Científicas y Técnicas of Argentina (CONICET), the Consejo de Investigaciones Científicas y Tecnológicas de la Provincia de Córdoba (CONICOR), and the Fundación Antorchas is gratefully acknowledged. S.L.C. thanks CONICET for the fellowship granted and TWAS for a travel fellowship. The authors also acknowledge helpful discussions with Dr. Garin and Dr. Zelada. The authors thank Miss L. P. Falcón for language assistance and Lic. Bonetto for performing SEM examination of samples.

References

1. J. B. Goodenough and J. M. Longo, *in* "Landolt–Börnstein New Series" (K. H. Hellwege and A. M. Hellwege, Eds.), Vol. 4, Part a, **p. 126,** Springer-Verlag, Berlin (1970).
2. F. S. Galasso, "Structure, Properties, and Preparation of Perovskite-Type Compounds," Pergamon, Oxford (1969).
3. J. B. Goodenough, *in* "Solid State Chemistry" (C. N. R. Rao, Ed.), Dekker, New York (1974).
4. R. E. Carbonio, C. Fierro, D. Tryk, D. Scherson, and E. Yeager, *J. Power Sources* **22,** 387 (1988).
5. R. J. Bouchard, J. F. Weiher, and J. L. Gillson, *J. Solid State Chem.* **6,** 519 (1973).
6. R. J. Bouchard, J. F. Weiher, and J. L. Gillson, *J. Solid State Chem.* **21,** 135 (1977).
7. T. C. Gibb, R. Greatrex, N. N. Greenwood, D. C. Puxley, and K. G. Snowdon, *J. Solid State Chem.* **11,** 17 (1974).
8. R. J. Bouchard and J. F. Weiher, *J. Solid State Chem.* **4,** 80 (1972).
9. M. Ceh, D. Kolar, and L. Golic, *J. Solid State Chem.* **68,** 68 (1987).
10. J. E. Sunstrom IV, S. M. Kauzlarich, and P. Klavins, *Chem. Mater.* **4,** 346 (1992).
11. A. Reller, *Ber. Bunsenges. Phys. Chem.* **90,** 742 (1986).
12. L. G. Tejuca, J. L. G. Fierro, and J. M. D. Tascón, *Adv. Cataly.* **36,** 237 (1989).
13. R. J. H. Voorhoeve, D. W., Jr. Johnson, J. P. Remeika, and P. K. Gallagher, *Science* **195,** 827 (1977).
14. R. J. H. Voorhoeve, *in* "Advanced Materials in Catalysis" (J. J. Burton and R. L. Garten, Eds.), Academic Press, New York (1977).
15. C. Fierro, R. E. Carbonio, D. Scherson, and E. Yeager, *Electrochim. Acta* **33,** 941 (1988).
16. Diffraction File No. 35-734.
17. W. Gong, H. Yun, Y. B. Ning, J. E. Greedan, W. R. Datars, and C. V. Stager, *J. Solid State Chem.* **90,** 320 (1991) and references therein.
18. A. L. Kholbin, E. V. Kuchis, and V. A. Trefakov, *Ferroelectrics* **83,** 135 (1988).
19. J. J. Randall and R. Ward, *J. Am. Chem. Soc.* **81,** 2629 (1959).
20. R. J. Bouchard and J. L. Gillson, *Mater. Res. Bull.* **7,** 873 (1972).
21. P. R. Van Loan, *Ceram. Bull.* **51,** 231 (1972).
22. C. W. Jones, P. D. Battle, P. Lightfoot, and W. T. A. Harrison, *Acta Crystallogr. Sect. C* **45,** 365 (1989).
23. T. C. Gibb, R. Greatrex, N. N. Greenwood, and K. G. Snowdon, *J. Solid State Chem.* **14,** 193 (1975).
24. J. M. Longo, P. M. Raccah, and J. B. Goodenough, *J. Appl. Phys.* **39,** 1327 (1968).
25. A. Callaghan, C. W. Moeller, and R. Ward, *Inorg. Chem.* **5,** 1572 (1966).
26. D. Telles, A. Hanmett, and J. B. Goodenough, "Localization and Metal–Insulator Transition" (H. Fritzsche and D. Adler, Eds.), Plenum, New York (1985).
27. J. B. Goodenough, "Metallic Oxides," Progress in solid state chemistry (H. Reiss Ed.), Vol. 5, Pergamon, Oxford (1971).
28. M. H. Mueller, L. Heaton, and K. T. Miller, *Acta Crystallogr.* **13,** 828 (1960).
29. K. Yvon, W. Jeitschko, and E. Parthe, *J. Appl. Crystallogr.* **10,** 73 (1977).
30. W. Bensch, H. W. Schmalle, and A. Reller, *Solid State Ionics* **43,** 171 (1990).
31. P. Ganguly and N. Y. Vasanthacharya, *J. Solid State Chem.* **61,** 164 (1986) and references therein.
32. S. D. Ross, "Inorganic Infrared and Raman Spectra," McGraw–Hill, London (1972).
33. N. F. Mott, *J. Phys. Les Ulis Fr.* **50,** 2811 (1989).
34. J. B. Goodenough, *J. Appl. Phys.* **37,** 1415 (1966).
35. J. B. Goodenough, *Bull. Soc. Chim. Fr.* **1200** (1965).

36. T. WOLFRAM, R. HURST, AND F. J. MORIN, *Phys. Rev. B* **15,** 1151 (1977).
37. F. P. KOFFYBERG, K. DWIGHT, AND A. WOLD, *Solid State Commun.* **30,** 433 (1979).
38. P. SALVADOR, C. GUTIERREZ, G. CAMPET, AND P. HAGENMÜLLER, *J. Electrochem. Soc.* **131,** 550 (1984).
39. A. KABANYASI, *J. Phys. Soc. Jpn.* **41,** 1876 (1976).
40. "International Tables for X-Ray Crystallography," Vol. IV, Kynoch, Birmingham (1976).